This article has been accepted for publication in a future issue of this journal, but has not been fully edited. Content may change prior to final publication. Citation information: DOI 10.1109/TAP.2017.2776346, IEEE Transactions on Antennas and Propagation

A Low Profile Dual-polarized High Isolation MIMO Antenna Arrays for Wideband Base Station Applications

Huiqing Zhai, *Member, IEEE,* Lei Xi, Yiping Zang, and Long Li, *Senior Member, IEEE*

Abstract—A low profile dual-polarized high isolation MIMO antenna arrays for wideband base station applications is presented in this paper. The proposed dual-polarized antenna element has the advantage of lower profile (0.067λ) by utilizing artificial magnetic conductor (AMC) structure. The antenna array consisting of four elements is working within the frequency band from 2.4GHz to 3.0GHz. Furthermore, decoupling branches among the elements are introduced to improve the isolation by about 10dB. Both simulated and measured results indicate that the proposed dual-polarized antenna element has a good isolation over 28dB. Moreover, the beam width of the antenna array can be effectively broadened by the adjustment of phase distributions of corresponding artificial material plane. Finally, a larger MIMO system is also investigated, and the simulated and measured results prove that dual-polarized dipole antenna MIMO array has good system performance.

***Index Terms*--Dual-polarized, low profile, high isolation, MIMO, AMC structure.**

I. Introduction

With the rapid technological development of wireless communication, frequency resources are facing a serious shortage problem. The demands for wireless communication are no longer limited to simple voice communication, while the demands for streaming media signal become more urgent. Therefore, how to make full use of limited spectrum resources to improve the transmission speed and the quality of the electromagnetic signal is of great significance. Dual-polarized antenna is an effective methodology to increase the frequency spectrum efficiency. Simultaneously, the antenna can not only ease the polarization mismatch between transmitter and receiver, but also deal with the problem of multipath fading. Moreover, dual-polarized antenna can effectively reduce the number of antennas and reduce overall costs.

Actually, the base station antenna is a key component of the mobile communication system, and its performance will directly affect the quality of the mobile communication network coverage. Currently, high integration degree of the base station antenna has attracted great attention. One of the key points is reducing the radiating elements cross-sectional height.

Multiple input multiple output (MIMO) technology can provide a new and effective method to solve the problem of higher communication capacity. Namely, at the sending and receiving ends of the link system, multiple antennas are used to form a multi-antenna transmitting and receiving mode. In the system, the capacity and spectral efficiency could be substantially improved without increasing the power and bandwidth of the device. Thus, the performance of MIMO antennas will be the one of key problems for affecting the overall system operation.

TABLE I
THE COMPARISON BETWEEN THIS PAPER AND REFERENCES

	height	polarization	bandwidth	S21	XP	efficiency
this paper	0.067λ	2	22.3%	30dB	23dB	92%
[1]	0.258λ	2	45%	30dB	23dB	40%
[10]	0.124λ	2	16.4%	35dB	21dB	45%
[13]	0.16λ	1	19.3%	none	18dB	none
[22]	0.126λ	2	18.6%	30dB	35dB	none

Typically, many new-designed antennas described in [1]–[10] have dual-polarized characteristics, high gain characteristics, and anti-multipath fading performance. Many proposed dual polarized antennas, such as ones with different heights in [1] (0.258λ),[4] (0.25λ), [8] (0.285λ), have wide bandwidth, low cross-polarization ratio and high port isolation. Other dual-polarized antennas with metal cavity have good back lobe with different heights in [2] (0.2λ), [3](0.256λ), [5] (0.264λ), [6] (0.288λ), and [7] (0.3λ). However, the most of above methods have increased the height of the antenna. An antenna array with multi-frequency and dual-polarized elements was provided in [9] (0.205λ). Another antenna adopts a metal cube in order to decrease the antenna height, while increasing the volume of the antenna in [10] (0.124λ). To reduce the height, researchers have presented many methods and new structures. The antennas described in [11]–[20] have lower profiles than the previous antennas. An AMC structure applied on the broadband monopole antenna with good radiation characteristics was proposed in [11], [12], [15], and [18-20]. Meanwhile, the multi-frequency circularly polarized metamaterial antennas were also shown in [13-14] and [16-17]. In [21-23], dual-polarized low profile antennas with AMC are proposed. The height of approximate 0.13λ of antennas is shown, but the works of antenna array are not involved. The woks in this paper are compared with the

This work is supported by the NSFC under Contract No. 51477126.

H. Zhai, L. Xi, Y. Zang, and L. Li are with National Key Laboratory on Antenna and Microwave Techniques, the School of Electronic Engineering, Xidian University, Xi'an, 710071, China.

This article has been accepted for publication in a future issue of this journal, but has not been fully edited. Content may change prior to final publication. Citation information: DOI 10.1109/TAP.2017.2776346, IEEE Transactions on Antennas and Propagation

references, as shown in Table I.

In this paper, a low profile dual-polarized high isolation antenna MIMO arrays for wideband base station applications is presented and discussed. The MIMO array is backed by a single-layer AMC structure with circle metallic unit cells, allowing the antenna to yield a low profile to achieve the unidirectional radiation. The primary radiation element consists of two spatial orthogonal dipoles for wide band operation. The lower profile is formed by the combination of inverted L-shaped feed and AMC in the MIMO array. Furthermore, decoupling structures on the AMC are introduced to reduce the couplings between dual-polarized antenna elements in MIMO array. The beam width of the present array antenna is also studied in Section II., in which the beam width can be broadened according to the phase reflection band gap of material elements. The proposed antenna array has been demonstrated by the simulation with the software HFSS and experiment.

II. Dipole Antenna Element Over AMC Surface

In this section, the characteristics of the dual-polarized dipole antenna element over AMC surface are discussed in detail, in which the results of S-parameters and pattern analysis for antenna element will be included. It is confirmed that the present antenna can achieve the low profile of 8mm (0.067λ) without substantially sacrificing other performances.

A. Dual-polarized Dipole Antenna Element Design over AMC Surface

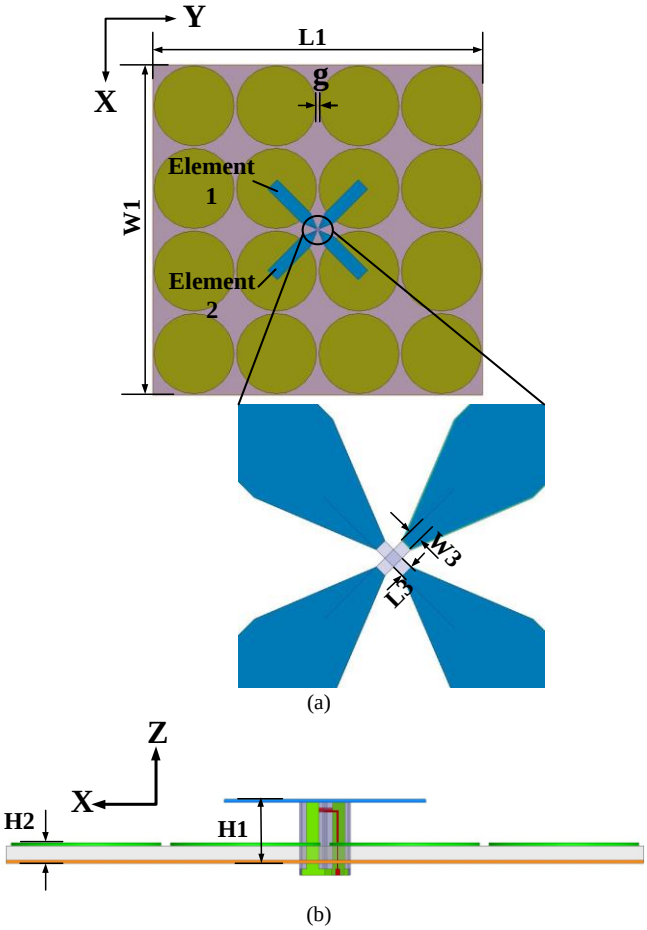

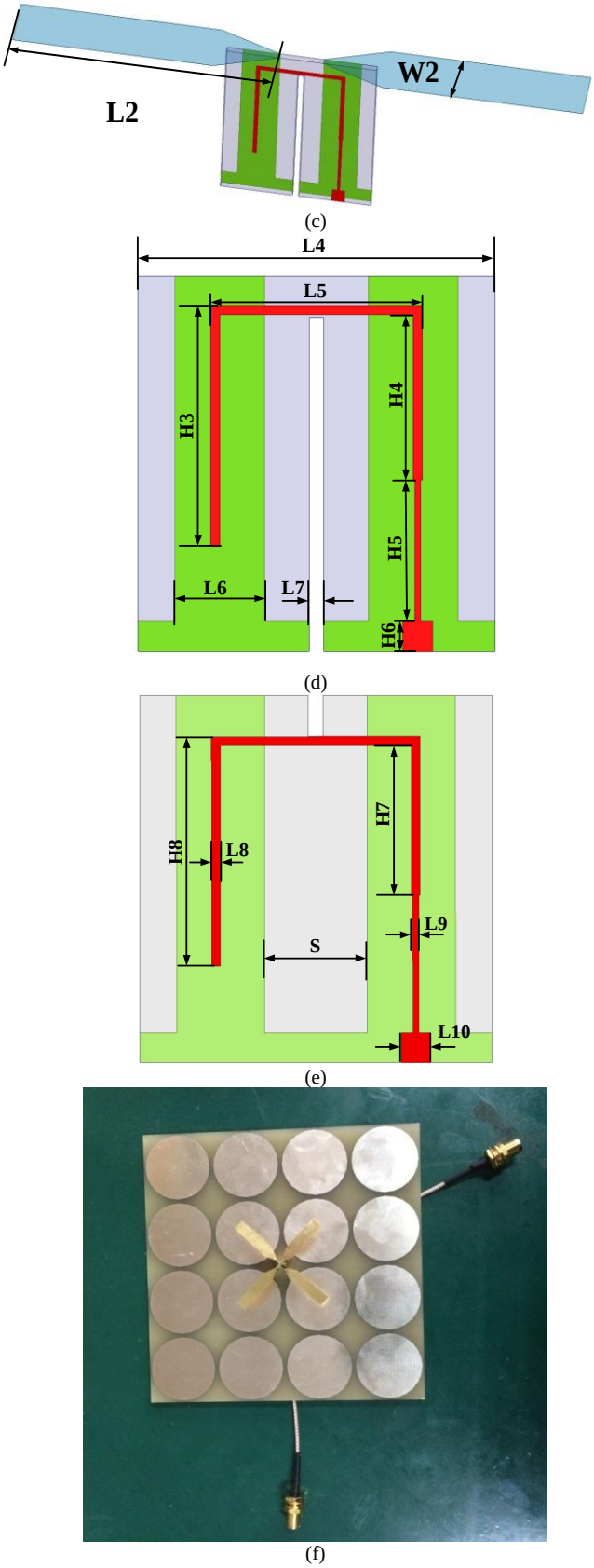

Fig. 1. The geometry of the proposed antenna over AMC surface. (a) The top view of the proposed antenna. (b) The side view of the proposed antenna. (c) The overall view of the element 1. (d) The structure of the feed lines for element 1.(e) The structure of the feed lines for element 2.(f) The fabricated photo of the dual-polarized antenna.

This article has been accepted for publication in a future issue of this journal, but has not been fully edited. Content may change prior to final publication. Citation information: DOI 10.1109/TAP.2017.2776346, IEEE Transactions on Antennas and Propagation

TABLE II
DIMENSIONS OF THE PROPOSED ANTENNA (UNIT: MM)

Parameter	L1	L2	L3	L4	L5	L6
Value	112	23	0.5	9	5.32	3
Parameter	L7	L8	L9	L10	W1	W2
Value	0.5	0.52	0.2	0.8	112	4.5
Parameter	W3	H1	H2	H3	H4	H5
Value	0.5	8	3	4.5	3.78	2.7
Parameter	H6	H7	H8	S		
Value	0.5	3.68	4.3	1.5		

The proposed dual-polarized dipole antenna element has two rectangle radiation patches, fed by two inverted L-shaped feedlines, whose perspective view is shown in Fig. 1 (a) and (b). This antenna consists of two orthogonal vertical substrates and AMC substrates shown in Fig.1 (d) and Fig. 1 (a), respectively. FR4whose dielectric constant is 4.4, and loss tangent is 0.02 is used for all the substrates. The two vertical feeding substrate patches are orthogonal to each other and they are over the AMC surface, plotted in Fig.1 (d). In Fig.1 (e), the constructions of the two vertical feeding substrate patches are drawn in detail. Moreover, the two rectangle patches and the two rectangular patches are symmetrical and the gap between them is S. Besides, one of the inverted L-shaped feeding lines in Fig.1 (a) is staggered at the middle of the feed point to physically isolate itself to the other one. The dimensions of proposed antenna are listed in Table II.

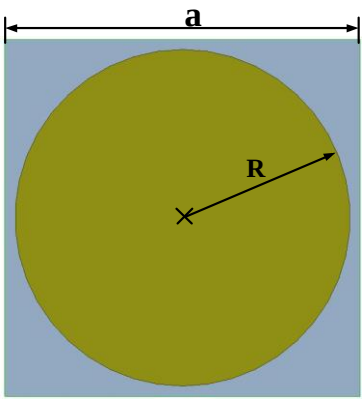

Fig. 2. The dimensions of the AMC cell.

The AMC cell consists of circle patch printed on a 3-mm-thick square FR4 substrate, as shown in Fig. 2. The circle patch has a radius of R=13.6mm, and the edge length of the AMC cell is expressed by a=28mm. The gap between adjacent AMC cells is defined as g=0.8mm, which is shown in Fig.1 (a).

B. Analysis of AMC Element

The surface has become a "magnetic conductor", because AMC structure is a high-impedance surface (HIS) composition [33]. On the surface, the tangential magnetic field is closed to zero. Impedance expressions take impedance surface located on XOY-plane and electromagnetic wave incident along the z-direction, the surface impedance is:

$$Z_S = \frac{E_y}{H_x} \tag{1}$$

Defining the incident electric and magnetic fields as E_i, H_i, reflection electric and magnetic fields are E_r, H_r.

Free space wave impedance expresses the relationship between the incident and reflected wave, and its expression is:

$$\left|\frac{E_i(z)}{H_i(z)}\right| = \left|\frac{E_r(z)}{H_r(z)}\right| = \sqrt{\frac{\mu_0}{\varepsilon_0}} = \eta_0 \tag{2}$$

The reflection phase of the surface can be drawn from above formula:

$$\phi = \mathrm{Im}[\ln(\frac{E_r}{E_i})] = \mathrm{Im}[\ln(\frac{Z_s - \eta_0}{Z_s + \eta_0})] \tag{3}$$

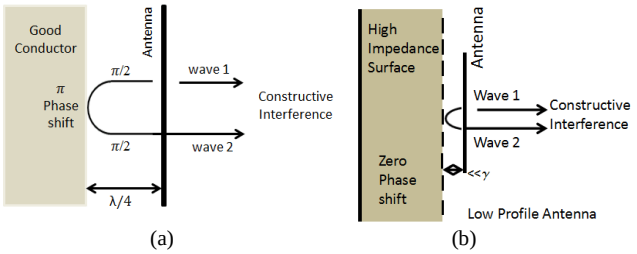

Fig. 3. The principle of plane wave reflection. (a) Metal surface reflection properties. (b) AMC surface reflection properties.

When Z_s is much smaller than η_0, the phase of reflection is about π. That is, after the surface reflection, electromagnetic field phase is the opposite, so the surface can be approximated as an ideal conductor surface. When Z_s is much larger than η_0, the phase of reflection is about 0. In this case, the surface can be approximated as an ideal magnetic conductor surface. Above two cased are shown in Fig.3.

Generally, the reflection phase of AMC ranging from -90 degrees to +90 degrees could be regarded as the in-phase reflection bandgap. The simulated in-phase reflection bandgap of the AMC is shown in Fig.4.

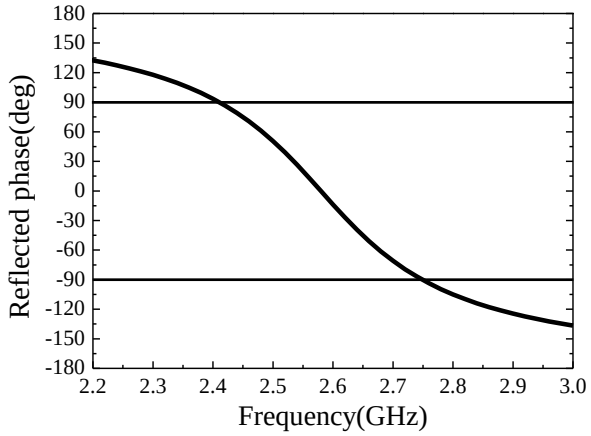

Fig. 4. The simulated reflection phase of the AMC.

C. Results and Discussions of Dipole Antenna Element over AMC Surface

The simulated and measured return losses of the proposed antenna and original dipoles without AMC for the two ports are shown in Fig. 5. The two antennas are working within the frequency band from 2.4GHz to 3.0GHz. Due to the small difference between the two inverted L-shaped feedlines, the operating frequency bands for port 1 and port 2 are slightly different. It can be seen that the simulated return losses for both ports are in good agreement with the measured ones. The

This article has been accepted for publication in a future issue of this journal, but has not been fully edited. Content may change prior to final publication. Citation information: DOI 10.1109/TAP.2017.2776346, IEEE Transactions on Antennas and Propagation

simulated and measured S_{12} of two antennas are shown in Fig. 6. It is observed that the port isolation of the proposed antenna is better than 28 dB in most of working band, which is also verified by simulated and measured results. There are some differences for S_{12} in high frequency, because the practical machining errors have not been fully considered. However, the port isolation of the original dipoles without AMC is worse than the proposed antenna. In a word, the radiation performance is not sacrificed substantially using the AMC configuration.

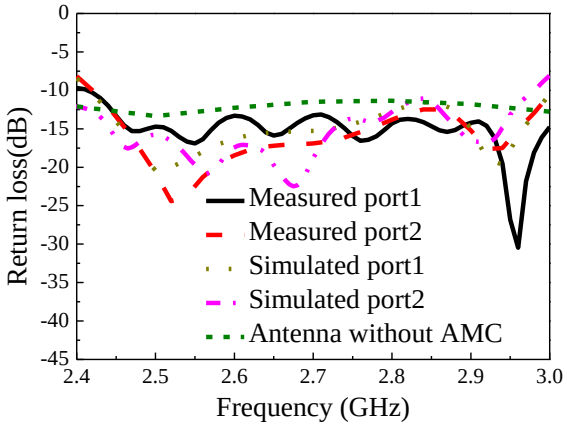

Fig. 5. Simulated and measured results of return losses of the proposed antenna and reference antenna.

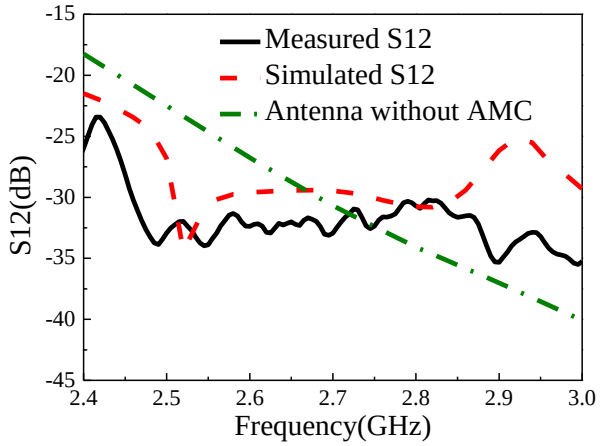

Fig. 6. Simulated and measured S_{12} of the proposed antenna and reference antenna.

The simulated and measured radiation patterns in E-plane and H-plane and measured cross-polarization of the antenna with and without AMC are drawn in Fig. 7. The patterns are approximately symmetrical, and maximum gains are in the direction of +*Z*. From Fig. 7, it can be seen that the radiation patterns in different frequencies remain stable. The gain for the port is higher than 7 dBi in most frequency. The specific values of beam width and cross polarization ratio are listed in Table III. It can be seen that antenna element has a good cross polarization ratio. And the 3 dB beam width is beyond 70 ° over the operating band. The radiation patterns of the antenna without AMC are shown in Fig. 7. It claims the radiation patterns are not influenced substantially using the AMC configuration. Furthermore, the antenna with AMC structure has a smaller back lobe than the one without AMC.

Some main parameters are investigated to understand the working states of the present antenna. Firstly, the research on inverted L-shaped feedline is carried out. The return losses of the analyses of L9 and H3 are drawn in Fig. 8 and Fig. 9, respectively. It can be seen that return losses become worse with the increase of parameter L9 and return losses become better with the increase of parameter H3. Hence, L9 and H3 are the important factors affecting the antenna impedance. Next, the dipole arm is explored. Fig. 10 shows the changes of return losses with the different lengths of the antenna arm L2. When the L2 increases, the frequency of the antenna moves to the high frequency and the bandwidth becomes narrow. According to the reasonable selections of parameters values, the better performances of the antenna could be obtained.

TABLE III
SPECIFIC VALUES OF BEAM WIDTH AND POLARIZATION

Frequency(GHz)	2.4	2.5	2.6	2.7	2.8	2.9	3.0
Beam width(deg)	71	74.5	71.6	70	155	109.1	110
cross-polarization ratio(dB)	23.5	21.7	25.4	26.4	27.5	22.1	18

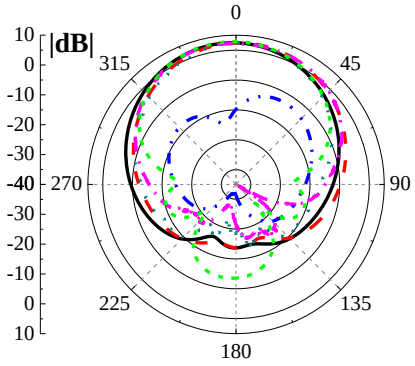

(a)

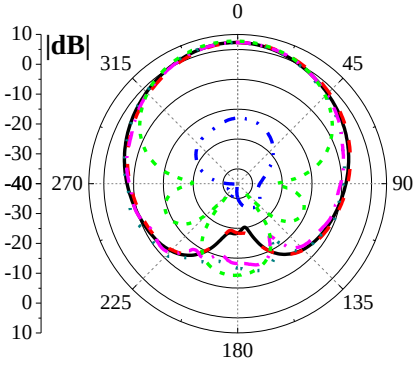

(b)

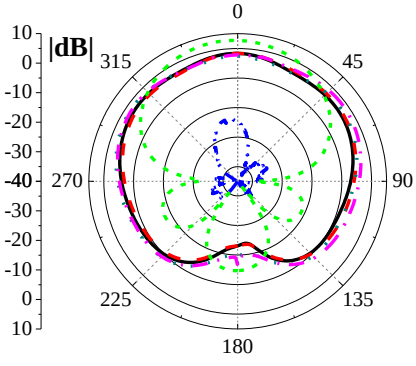

(c)

This article has been accepted for publication in a future issue of this journal, but has not been fully edited. Content may change prior to final publication. Citation information: DOI 10.1109/TAP.2017.2776346, IEEE Transactions on Antennas and Propagation

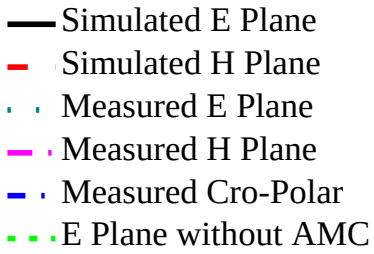

Fig. 7. Simulated and measured radiation patterns in E-plane and H –plane. (a) 2.5GHz. (b) 2.7GHz. (c) 2.9GHz.

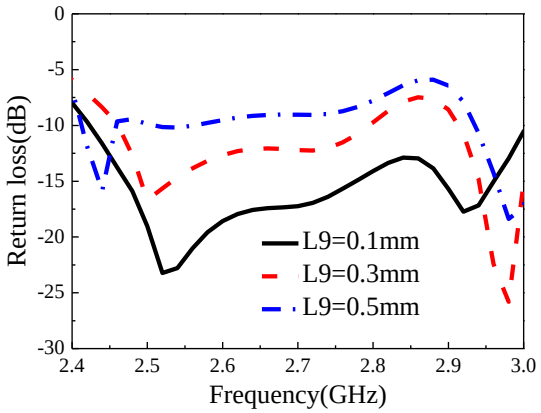

Fig. 8. The return losses of the proposed antenna for port 1 with the variation of L9.

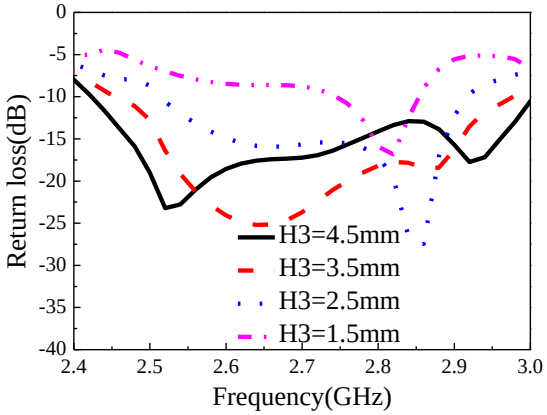

Fig. 9. The return losses of the proposed antenna for port 1 with the variation of H3.

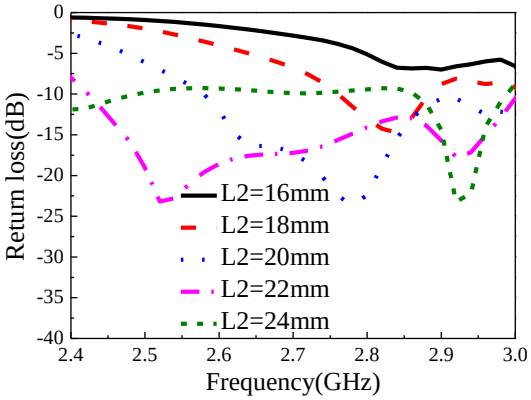

Fig. 10. The returns losses of the proposed antenna for port 1 with the variation of L2.

III. Dual Polarized Antenna Array Design For MIMO Applications

The proposed AMC antenna has the advantages of small size, low profile, wide bandwidth, and stable radiation pattern. Based on above antenna element, the high performance of the MIMO array will be studied in the following.

A. Dual-polarized Dipole Antenna Array Design over AMC Surface

Four dipole antennas, described above, are employed to develop the proposed four-element antenna array. The over view of the simulated antenna array model is shown in Fig. 11(a). The dimensions of the four-element antenna array are set as $112\times364\times12$ mm^3. The distance between antennas is d=84mm. Two one-four Wilkinson power dividers are used to connect to the dual polarization antenna array under the FR4 board, as shown in Fig. 11(b). The top view and bottom view of fabricated antenna array model are also shown in Fig. 11(c) and Fig. 11(d).

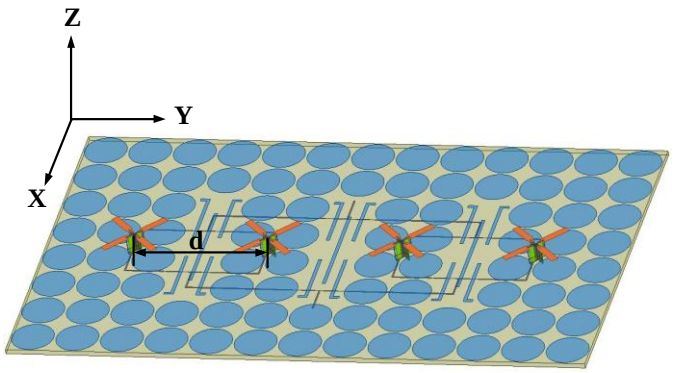

(a)

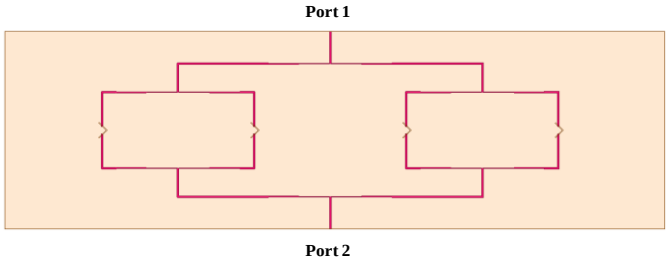

(b)

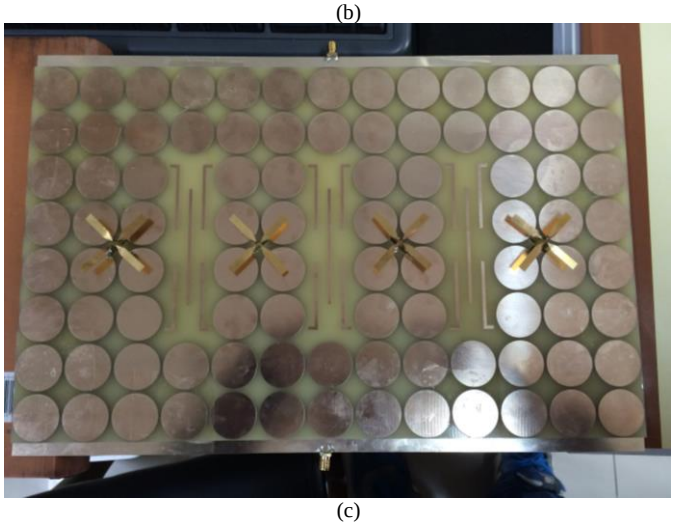

(c)

This article has been accepted for publication in a future issue of this journal, but has not been fully edited. Content may change prior to final publication. Citation information: DOI 10.1109/TAP.2017.2776346, IEEE Transactions on Antennas and Propagation

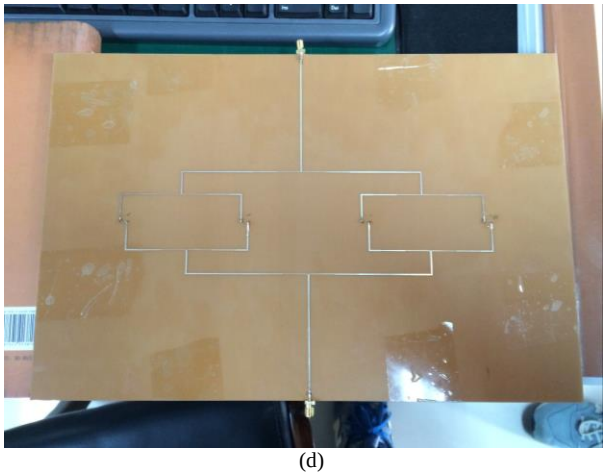

(d)

Fig. 11. (a) The over view of the simulated antenna array model. (b) The bottom view of the simulated antenna array model for feed network. (c) The top view of the fabricated antenna array. (d) The bottom view of the fabricated antenna array including power dividers.

B. Results and Discussions of Dual-Polarized Antenna Array over AMC Surface

The simulated and measured return losses for the two ports are given in Fig. 12. It can be seen that the simulated and measured return losses for both ports are in good agreement, ranging from 2.35 GHz to 3.0 GHz. The simulated and measured S_{12} are shown in Fig. 13. It is observed clearly that the measured and simulated S_{12} results are less than -28dB over the entire operating frequency band.

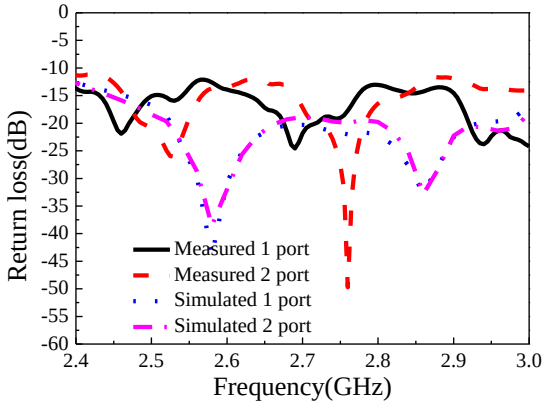

Fig. 12. Simulated and measured results of return losses for port1 and port2 in operating frequency band.

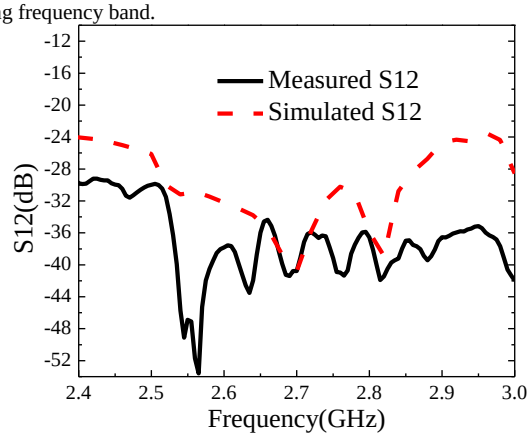

Fig. 13. Simulated and measured results of S_{12} for two array ports on operating frequency.

Actually, in order to achieve higher isolations, the decoupling branch is introduced [34] on the top surface of AMC structure, which is shown in Fig.14. The dimensions of the decoupling branch are also given in detail.

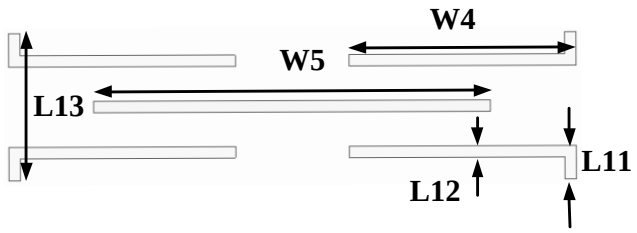

Fig.14. The dimension of decoupling branch. W4=40, W5=70, L11=6, L12=2, L13=26; Unit: mm.

The results of S_{12} between the two ports of the antenna arrays with and without decoupling branches are described in Fig.15. From the comparison, it is clearly seen that the isolation between two ports can be improved by 10dB under the use of the present decoupling branches.

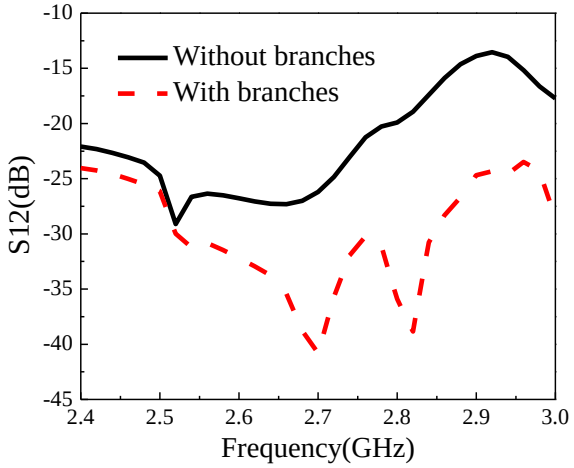

Fig. 15. The results of $S_{12}$with and without decoupling branches.

In order to explain the decoupling mechanism of the introduced decoupling branches, the current distributions with and without decoupling branches at the center frequency (2.6GHz) are shown in Fig.16. The left side of the figure is a transmitting antenna, and the right side is receiving antennas. It is obvious that the coupled energy is greatly reduced after adopting the decoupling branch according to the current distribution comparison of the receiving antennas. Actually, the decoupling branch in Fig.16 (b) works as a resonator and it acts like a barrier between transmitting antenna and receiving antenna. It can be concluded that the isolation could be greatly improved by the introduced decoupling branches.

The simulated and measured radiation patterns in XOZ/YOZ-plane at the different working frequencies are drawn in Fig.17. The patterns are approximately symmetrical in XOZ/YOZ-plane, and maximum gains are in the direction of +Z. The half power beam width is as wide as 93° in XOZ-Plane and the half power beam width is as wide as 20° in YOZ-Plane. From the results of simulated and measured

This article has been accepted for publication in a future issue of this journal, but has not been fully edited. Content may change prior to final publication. Citation information: DOI 10.1109/TAP.2017.2776346, IEEE Transactions on Antennas and Propagation

patterns, it can be seen that the radiation patterns in different frequencies remain stable. The measured co-polarization and cross-polarization of antenna array are described in Fig.18. A good cross polarization ratio of approximately 20 dB of the antenna array can be seen, which ensures the good radiation of the antenna in the direction of the main polarization. The simulated and measured gains and radiation efficiency of antenna array are shown in Fig. 19. The gains for the two ports are over 10.2dBi and the radiation efficiency of antenna array can reach beyond 82% at the working frequencies.

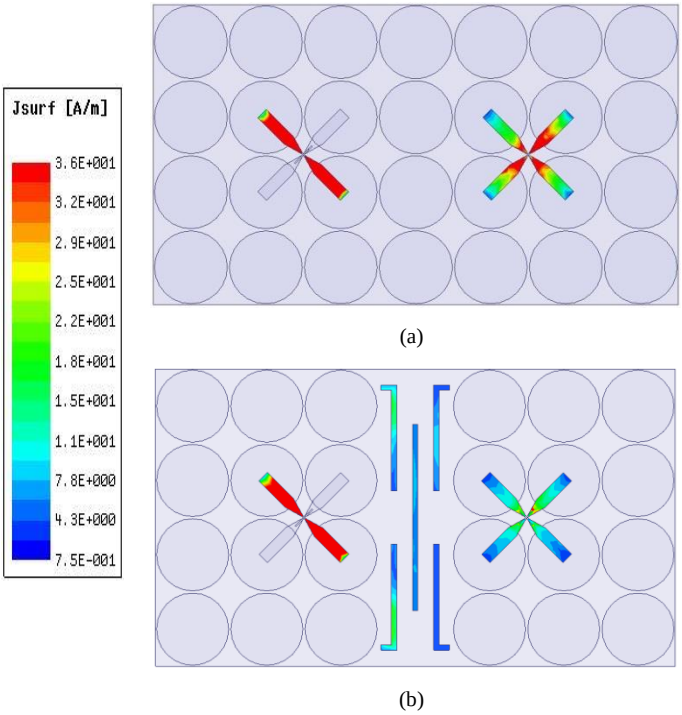

Fig.16. The current distributions of the antenna array. (a) The array antennas without branch. (b) The array antennas with branch.

The far field of fabricated antenna array (1×4) is measured in an anechoic chamber, which is shown in Fig.20.

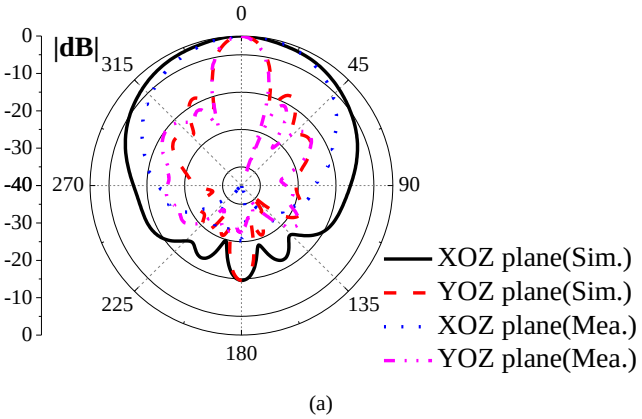

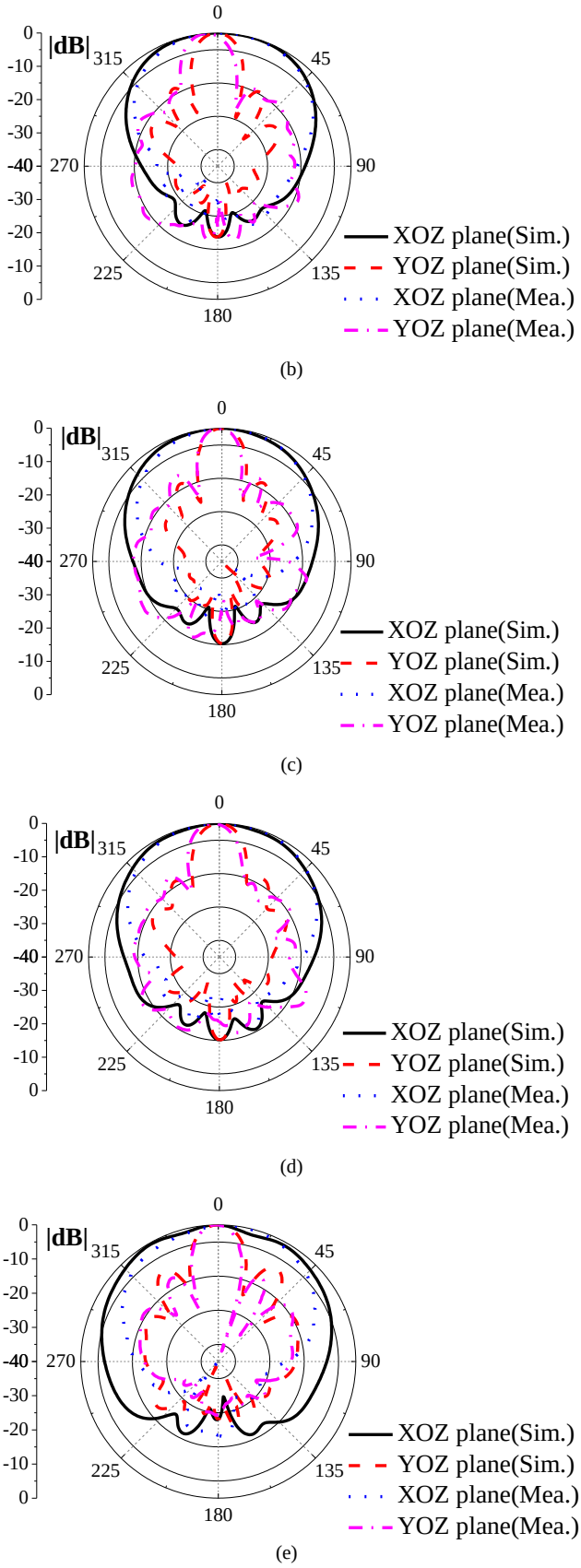

Fig.17. The simulated and measured patterns in XOZ-plane and YOZ-plane patterns. (a) 2.4GHz. (b) 2.5GHz. (c) 2.6GHz. (d) 2.7GHz. (e) 3.0GHz.

This article has been accepted for publication in a future issue of this journal, but has not been fully edited. Content may change prior to final publication. Citation information: DOI 10.1109/TAP.2017.2776346, IEEE Transactions on Antennas and Propagation

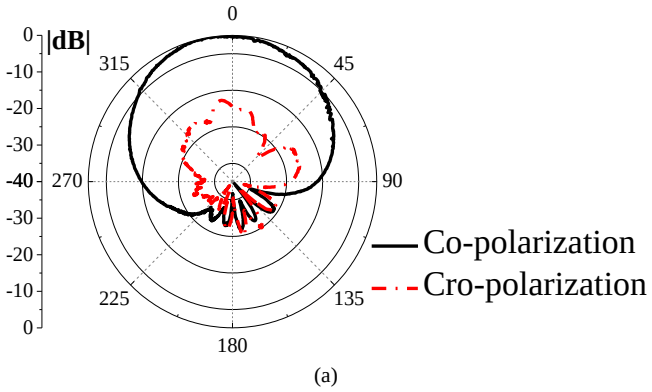

(a)

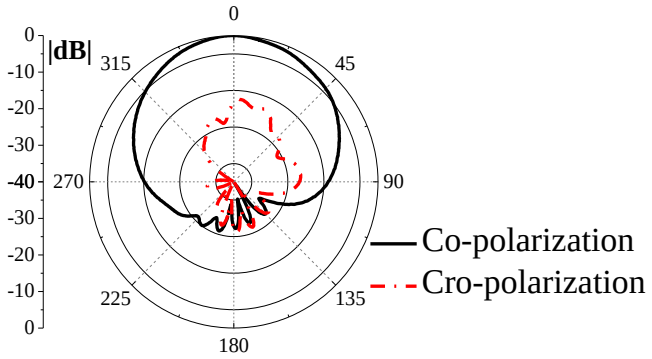

(b)

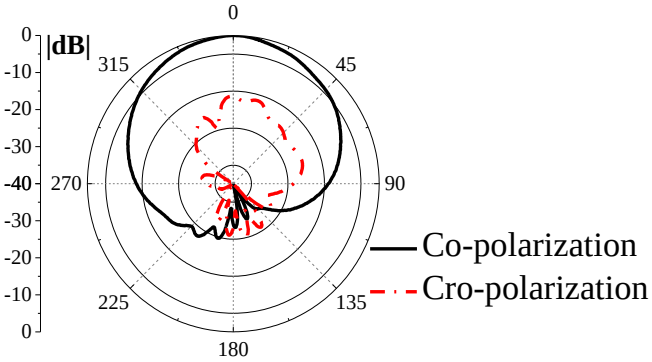

(c)

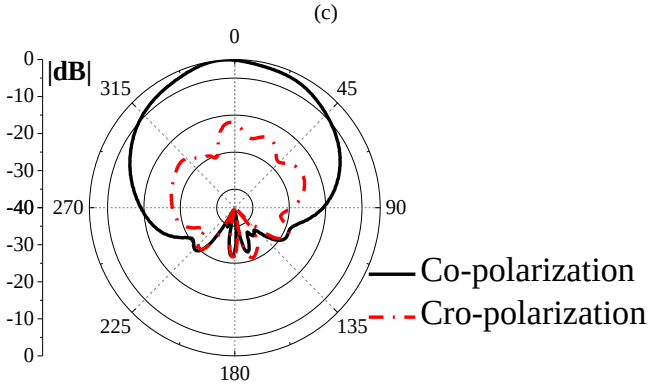

(d)

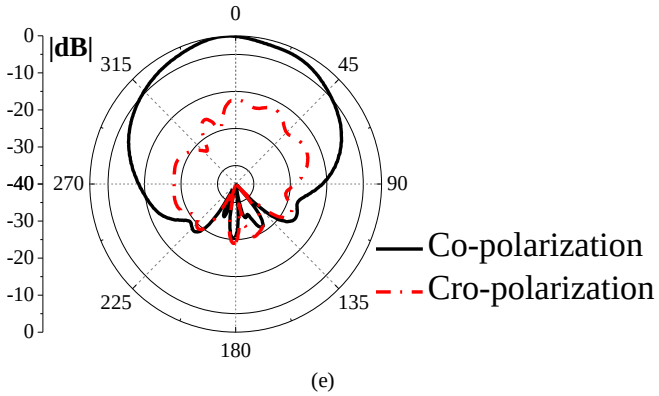

(e)

Fig. 18. The measured ratio of cross polarization of antenna array. (a) 2.4GHz. (b) 2.5GHz. (c) 2.6GHz. (d) 2.7GHz. (e) 3.0GHz.

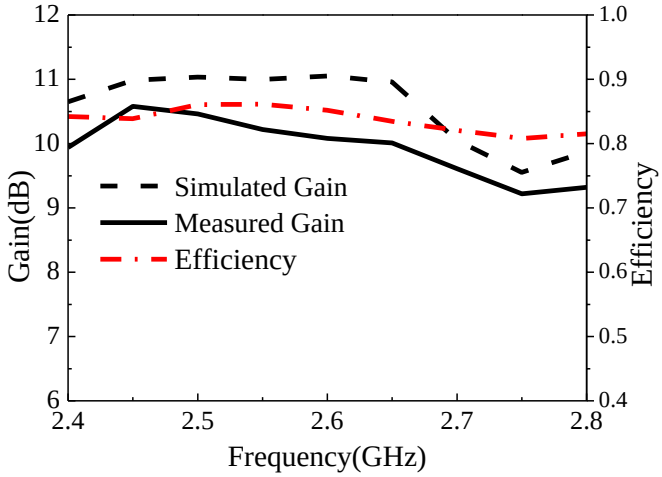

Fig.19. The gains and efficiency of antenna array.

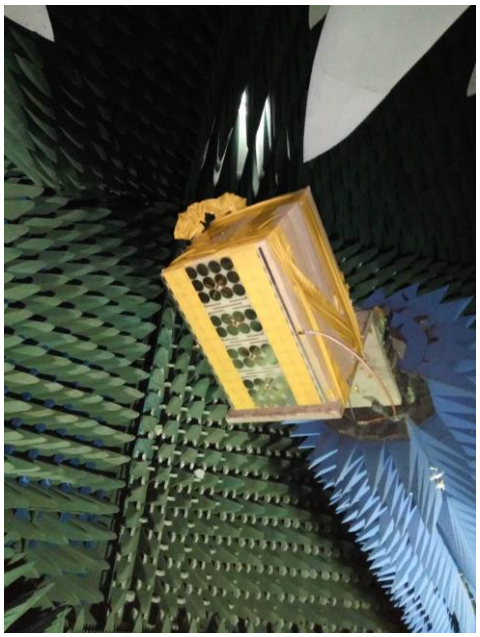

Fig.20. The far field test in an anechoic chamber.

This article has been accepted for publication in a future issue of this journal, but has not been fully edited. Content may change prior to final publication. Citation information: DOI 10.1109/TAP.2017.2776346, IEEE Transactions on Antennas and Propagation

C. Designs and Discussions of enhancing Dual-Polarized Antenna Array Beam Width

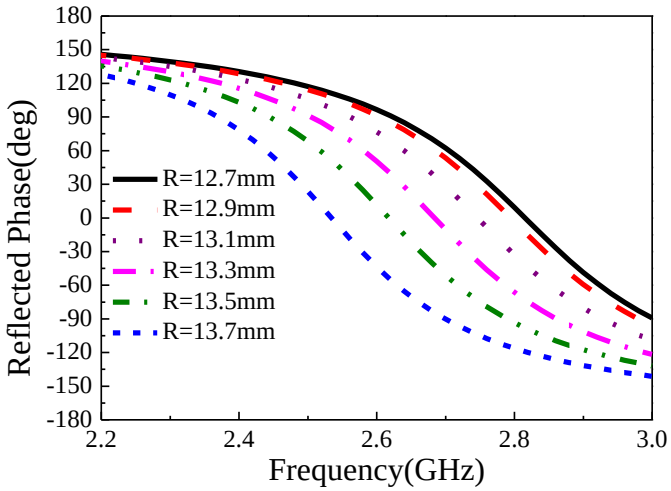

Fig.21. The reflected phase curves with the varying R.

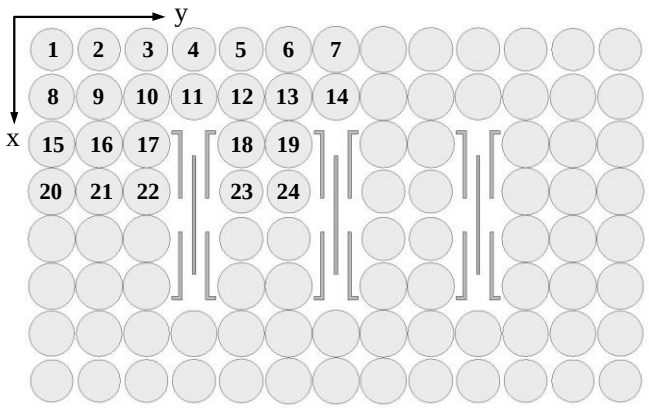

Fig.22. The surface distributions of metamaterial reflected array.

TABLE IV
VALUES OF CIRCLE RADIUS (UNIT: MM)

R1	R2	R3	R4	R5	R6
12.5	12.55	12.7	12.85	12.99	13.64
R7	R8	R9	R10	R11	R12
13.69	13.4	13.53	13.6	13.66	13.69
R13	R14	R15	R16	R17	R18
13.92	13.84	13.73	13.91	13.91	13.95
R19	R20	R21	R22	R23	R24
13.95	13.92	13.85	13.95	12.78	12.78

Beam width is a key parameter of communication base station antenna, which can effectively control communication area size. Here, the study on beam width of the low profile dual-polarized array will be carried out in the following.

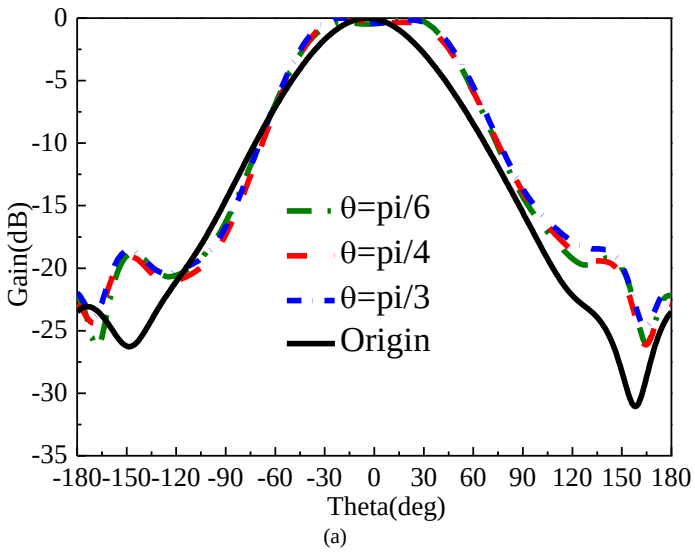

(a)

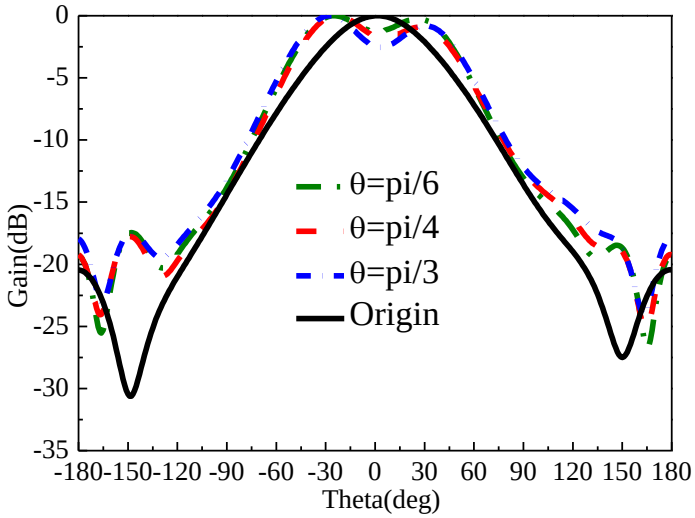

(b)

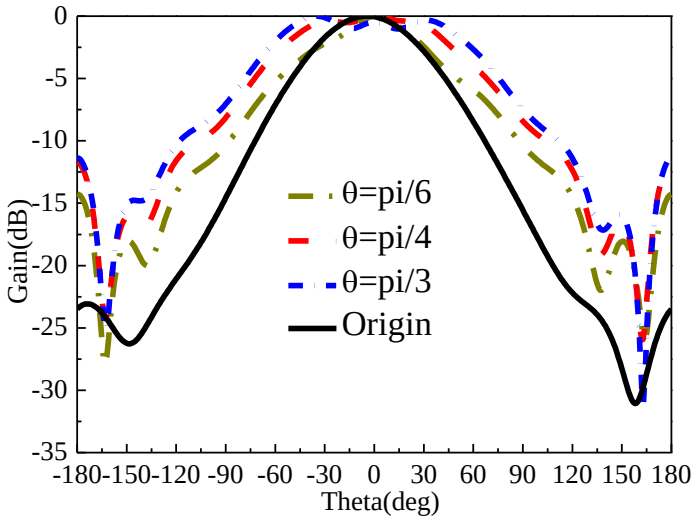

(c)

This article has been accepted for publication in a future issue of this journal, but has not been fully edited. Content may change prior to final publication. Citation information: DOI 10.1109/TAP.2017.2776346, IEEE Transactions on Antennas and Propagation

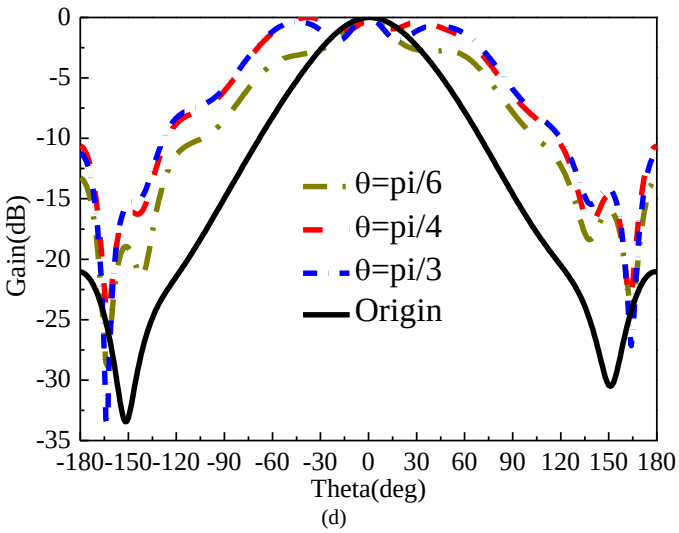

(d)

Fig.23. The compared patterns with the varying AMC. (a) 2.4GHz. (b) 2.5GHz. (c) 2.6GHz. (c) 2.65GHz.

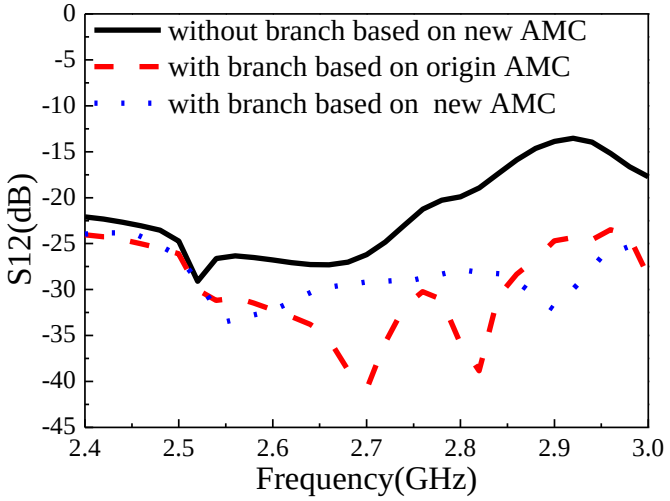

Fig.24. The compared port isolations of antenna array.

Without increasing the antenna array profile and size, the beam width could be broadened according to the phase distributions of metamaterial elements. According to changing the radius R of AMC element, metamaterial reflection bandgap can be adjusted. The results of reflected phase with the radius R are shown in Fig.21. The results describe that the reflection phases move towards the lower frequency when the R increases. The surface distributions of metamaterial reflected array is given in Fig. 22. MATLAB software is adopted to calculate the required radius value of each circle for reflected phase. This method is based on the principle of reflection array to extend the beam. There is an important parameter θ, which is the angle of the 1/4 area AMC reflection beam. Meanwhile, Fig. 23 describes the beam width of antenna array adopted the metamaterial reflection phase distributions. From the figure, it can be seen that the beam width can be gradually increased from pi/6 to pi/3. The compared port isolations of antenna array using reflection array is given in Fig. 24. In the use of beam broadening technology, the port isolation of antenna array is consistent with previous antenna array adopting the decoupling branch, that is less than -28dB.

As the circles of AMC are symmetrical about the center, the radiuses of 1/4 are given in Table IV with the angle of the AMC reflection beam θ=pi/3.

From above results, it is clearly shown that the beam widths can be effectively broadened in working band. Specifically, the beam width can be broadened from 99 degrees to 146 degrees within the frequency band from 2.4GHz to 2.65GHz.

D. Dual-polarized Dipole Antenna Array for MIMO Applications

The MIMO technology without increasing bandwidth can exponentially increase the transmission rate, spectrum efficiency, and further channel capacity. MIMO antenna technology has become an important component of a wireless communication system.

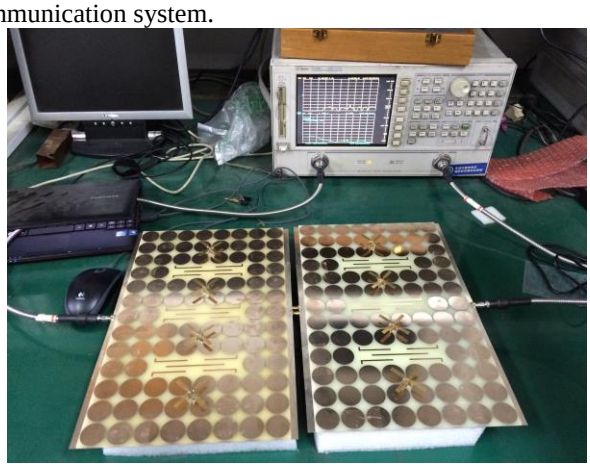

Fig.25. The experimental measurement for 2×4MIMO array system.

Mutual coupling analysis becomes an indispensable part for MIMO systems. It is directly related to the communication quality of MIMO system. Here is the mutual coupling parameter of envelope correlation coefficient (ECC)[27]:

$$\rho_e = \frac{\left|\eta_1 \cdot S_{11}^* \cdot S_{12} + \eta_2 \cdot S_{21}^* \cdot S_{22}\right|^2}{\left(\eta_1 - \eta_1 \cdot \left|S_{11}\right|^2 + \eta_2 \cdot \left|S_{21}\right|^2\right)\left(\eta_2 - \eta_2 \cdot \left|S_{22}\right|^2 + \eta_1 \cdot \left|S_{12}\right|^2\right)} \quad (4)$$

where η_1 and η_2 are the radiation efficiencies of the two antennas respectively. Meanwhile, S_{ii} is the reflection coefficient for the *i*th-port, and S_{ij} is the transmission coefficient from *j*th-port to *i*th-port.

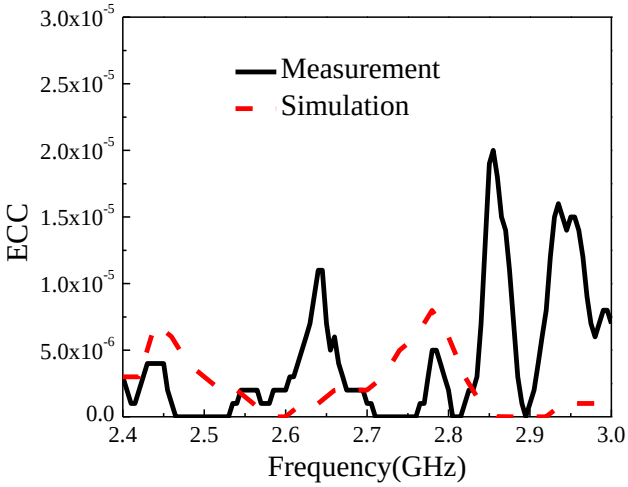

Fig.26. Simulated and measured results of the ECC for 2×4 MIMO array system.

Here, the dual-MIMO experiment is also investigated in the section. The 2×4 MIMO antenna array is measured, as shown in Fig.25. A comparison of the measured and simulation results of the ECC for 2×4 MIMO array system are described in Fig.26. It is clearly that the ECC is far less than 0.5, which indicates the proposed antenna array could be a better candidate for the base station MIMO terminal system.

IV. Conclusion

A new low profile dual-polarized enhanced beam high isolation antenna MIMO arrays for wideband base station applications is designed. The AMC surface plays a key role in antenna miniaturization and low profile, and the proposed MIMO antennas have the advantages of high isolation, dual polarization, wide coverage area, and good radiation performance. Experimental results certify that the proposed dual-polarized dipole antenna achieves isolation better than 28 dB within working band. Moreover, the beam width could be broadened according to the phase distributions of metamaterial elements. The present MIMO antenna array is suitable for wideband base station applications covering LTE, WLAN and WiMAX.

V. References

[1]Y. Y. Jin, and Z. W. Du, "Broadband Dual-Polarized F-Probe Fed Stacked Patch Antenna for Base Stations," *IEEE Antennas Wireless Propag. Lett*., vol. 14, pp. 1121–1124, Jan. 2015.

[2] A. Elsherbini, J. F. Wu, and K. Sarabandi, "Dual Polarized Wideband Directional Coupled Sectorial Loop Antennas for Radar and Mobile Base-Station Applications," *IEEE Trans. Antennas Propag*., vol. 63, no. 4, pp. 1505–1513, Apr. 2015.

[3] Q. X. Chu, D. L. Wen, and Y. Luo, "A Broadband ±45° Dual-Polarized Antenna With Y-Shaped Feeding Lines," *IEEE Trans. Antennas Propag*., vol. 63, no. 2, pp. 483–490, Feb. 2015.

[4] Y. Sh. Gou, S. W. Yang, and J. X. Li, "A Compact Dual-Polarized Printed Dipole Antenna With High Isolation for Wideband Base Station Applications," *IEEE Trans. Antennas Propag*., vol. 62, no. 8, pp. 4392–4395, Aug. 2014.

[5] Y. H. Cui, R. L. Li, and H. Z. Fu, "A Broadband Dual-Polarized Planar Antenna for 2G/3G/LTE Base Stations," *IEEE Trans. Antennas Propag*., vol.62, no. 9, pp.4836–4840,Sept.2014.

[6]Z. D. Bao, Z. P. Nie, and X. Z. Zong, "A Broadband Dual-Polarization Antenna Element for Wireless Communication Base Station," *IEEE Asia-Pacific Conference on Antennas and Propagation*.,pp.144–146, Aug. 2012.

[7] Z. Y. Zhang, J. Y. Zhao, and Q. Q. Liu, "Dual-Polarized Cross Bowtie Dipole for 3G and LTE Applications," *International Journal of Antennas and Propagation*.,vol. 2013, pp. 1-6,Oct. 2013.

[8] A. K. Arya, N. V. Anh, and R. S. Aziz, "Dual Polarized Dual Antennas for1.7–2.1 GHz LTE Base Stations," *IEEE Antennas Wireless Propag. Lett*., vol. 14, pp. 1427–1430, Mar.2015.

[9] Y. B. Jung, and S. Y. Eom, "A Compact MultiBand and Dual-Polarized Mobile Base-Station Antenna Using Optimal Array Structure," *International Journal of Antennas and Propagation*., vol. 2015, pp. 1-11, Apr, 2015.

[10] J. N. Lee, K. C. Lee, and P. J. Song, "The Design of a Dual-Polarized Small Base Station Antenna With High Isolation Having a Metallic Cube," *IEEE Trans. Antennas Propag*., vol. 63, no. 2, pp.791–795, Feb. 2015.

[11]G. H. Li, H. Q. Zhai, and L, Li, "AMC-Loaded Wideband Base Station Antenna for Indoor Access Point in MIMO System," *IEEE Trans. Antennas Propag*., vol. 63, no. 2, pp. 525–532, Feb. 2012.

[12]I. T. McMichael, A. I. Zaghloul, and M. S. Mirotznik, "A Method for Determining Optimal EBG Reflection Phase for Low Profile Dipole Antennas," *IEEE Trans. Antennas Propag*., vol. 61, no. 5, pp. 2411–2417, May. 2013.

[13] H. H. Tran, and I. Park, "A Dual-Wideband Circularly Polarized Antenna Using an Artificial Magnetic Conductor," *IEEE Antennas Wireless Propag. Lett*.,vol. 15, pp. 1–4, Apr. 2015.

[14] S. X. Ta, I. Park, and R. W. Ziolkowski, "Circularly Polarized Crossed Dipole on an HIS for 2.4/5.2/5.8-GHz WLAN Applications," *IEEE Antennas Wireless Propag. Lett*., vol. 12, pp. 1464–1467, Aug. 2013.

[15] H. R. Raad, A. I. Abbosh, and H. M. Al-Rizzo, "Flexible and Compact AMC Based Antenna for Telemedicine Applications," *IEEE Trans. Antennas Propag*., vol. 61, no. 2, pp. 524–531, Feb. 2013.

[16] S. Yan, P. J. Soh, and M. Mercuri, "Low Profile Dual-band Antenna Loaded with Artificial Magnetic Conductor for Indoor Radar Systems," *Special Issue on Application of Radar to Remote Patient Monitoring and Eldercare*., pp. 184–190, Aug.2014.

[17] H. Yi, and S. W. Qu, "A Novel Dual-Band Circularly Polarized Antenna Based on Electromagnetic Band-Gap Structure," *IEEE Antennas WirelessPropag. Lett*., vol. 12, pp. 1149–1152, Sept. 2013.

[18] W. Yang, H. Wang, W. Che, and J. Wang, "A Wideband and High-Gain Edge-Fed Patch Antenna and Array Using Artificial Magnetic Conductor Structures," *IEEE Antennas WirelessPropag. Lett*., vol. 12, pp. 769–772, Jun. 2013.

[19]D. Cure, T. Weller, and F. Miranda, "Study of a Flexible Low Profile Tunable Dipole Antenna Using Barium Strontium TitanateVaractors," *European Conference on Antennas and Propagation*.,pp.31-35, Sept.2014.

[20]N. M. Mohamed-Hicho,E.Antonino-Daviu, and M. Cabedo-Fabrés, "A Novel Low-Profile High-Gain UHF Antenna Using High-Impedance Surfaces," *IEEE Antennas Wireless Propag. Lett*., vol. 14.no. 9,pp. 1014-1017, Oct.2015.

[21] J. Ren, B. Wang, and Y. Z. Yin, "Low Profile Dual-Polarized Circular Patch Antenna with an AMC Reflector," *Progress In Electromagnetics Research Letters*.,vol. 28.no. 8,pp. 956–962, Feb.2014.

[22] B. Li, W. Hu, J. Ren, and Y. Z. Yin, "Low-Profile Dual-Polarized Patch Antenna with HIS Reflector for Base Station Application," *Journal of Electromagnetic Waves and Applications*.,vol. 47. pp. 131–137, Aug.2014.

[23] W. Hu, R. N. Lian, Z. Y. Tang, and Y. Z. Yin, "Wideband, Low-Profile, Dual-Polarized Slot Antenna with an AMC Surface for Wireless Communications," *Progress In Electromagnetics Research Letters*.,vol. 2016. pp. 1–8, Oct.2016.

[24] X. Liu, S. H. He, and H. M. Zhou, "A Novel Low-Profile, Dual-Band, Dual-Polarization Broadband Array Antenna for 2G/3G Base Station," *International Conference on Wireless*., pp. 1–4, Aug.2006.

[25] J. Kim, J. Ju, S. Eom, M. Song, and N. Kim, "Four-Channel MIMO Antenna for WLAN Using Hybrid Structure," *Electron Lett*., vol. 49, no. 14, pp. 857–858, Jul. 2013.

[26]L. Liu, S. W. Cheung, and T. I. Yuk, "Compact MIMO Antenna for Portable Devices in UWB Applications," *IEEE Trans. Antennas Propag*., vol. 61, no. 8, pp. 4257–4264, Aug. 2013.

[27]S. W. Su, "High-Gain Dual-Loop Antennas for MIMO Access Points in the 2.4/5.2/5.8 GHz Bands," *IEEE Trans. Antennas Propag*., vol. 58, no. 7, pp. 2412–2419, Jul. 2010.

[28] H. Nakano, Y. Ogino, and J. Yamauchi, "Bent Two-Leaf Antenna Radiating a Tilted, Linearly Polarized, Wide Beam," *IEEE Trans. Antennas Propag*., vol. 58, no. 11. pp. 3721–3725, Nov. 2010.

[29] S. X. Ta, H. Choo, I. Park, and R.W. Ziolkowski, "Multi-Band, Wide-Beam, Circularly Polarized, Crossed, Asymmetrically Barbed Dipole Antennas for GPS Applications," *IEEE Trans. Antennas Propag*., vol. 61, no. 11. pp. 5771–5775, Nov. 2013.

[30] H. Paul, "The Significance of Radiation Efficiencies When Using S-Parameters to Calculate the Received Signal Correlation From Two Antennas," *IEEE Antennas Wireless Propag. Lett*., vol. 4, pp.97–99, 2005.

[31] S. Raman, P.Mohanan, N. Timmons, and J.Morrison, "Microstrip-Fed Pattern- and Polarization-Reconfigurable Compact Truncated Monopole Antenna," *IEEE Antennas Wireless Propag. Lett*., vol. 12, pp. 710–713,May.2013.

[32] K. Kandasamy, B. Majumder, and J. Mukherjee, "Beam-Tilted and Wide Beam Antennas using Hybrid Electromagnetic Band Gap Structures," *European Microwave Conference*., pp.458-461,Dec.2015.

[33] A. Vallecchi, J. R,De Luis, F. Capolino, and F. D. Flaviis, "Low Profile Fully Planar Folded Dipole Antenna on a High Impedance Surface," *IEEE Trans. Antennas Propag*., vol. 60, no. 1, pp. 1505–1513, Jan. 2012.

[34] H. Wong, K. L. Lau, and K. W. Luk, "Design of Dual-Polarized L-Probe Patch Antenna Arrays with High Isolation," *IEEE Trans. Antennas Propag*., vol. 52, no. 1. pp. 45–52, Jan. 2004.

This article has been accepted for publication in a future issue of this journal, but has not been fully edited. Content may change prior to final publication. Citation information: DOI 10.1109/TAP.2017.2776346, IEEE Transactions on Antennas and Propagation

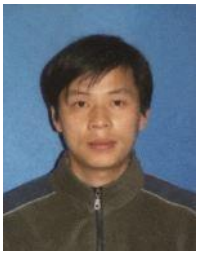

Huiqing Zhai (M'12) was born in Jilin province, China. He received the Ph.D. degrees in electromagnetic fields and microwave technology from Xidian University, Xi'an, China, in 2004.

He is a full professor and Ph.D supervisor with Xidian University. He received the Ph.D. degrees in electromagnetic fields and microwave technology from Xidian University, Xi'an, China, in 2004. From April 2005 to March 2008, he worked at Tohoku University, Sendai, Japan, as a JSPS Research Fellow. From July 2008 to May 2010, he worked at the University of Texas at Arlington, TX, USA, as a research fellow. His primary research interests include antennas for wireless communication, electromagnetic materials, electromagnetic detection and electromagnetic invisibility cloaking.

He has authors or coauthored over 100 papers in referred journal, and over 10 authorized invention patents. He achieved First Prize of Awards for Scientific Research Results of High Education of Shaanxi Province awarded by Education Department of Shaanxi Provincial Government in 2013, the Best Technical Cooperation Project Award of Huawei Corporation in 2014, and Second Prize of Awards of Science and Technology awarded by Shaanxi Province Government in 2016. He received the Japan Society for Promotion of Science Research Fellowship from April 2006 to March 2008. He won the Best Paper Award from the Institute of Electronics Information and Communication Engineers in 2009. He has been the deputy director of Microwave Telecommunication Engineering Department in Xidian University since 2016.

Lei Xi was born in Weinan, China, in 1992. He received the bachelor's degree in electronic and information engineering from Xidian University, Xi'an, China, in 2014. He is currently pursuing the Ph.D degree in electromagnetic field and microwave technology at Xidian University.

His research interests include electromagnetic metamaterial, circularly polarized antennas, dual-polarized antennas, filtering antenna, and MIMO antenna arrays.

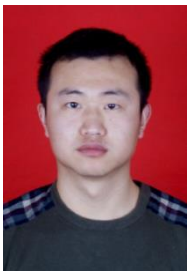

Yiping Zang received the B.S. degree in Optical Information Science and Technology from Chang'an College of Xidian University, Xi'an, China, in 2012.

He is currently pursuing the Ph.D. degree in Electromagnetic field and Microwave Technology from the Xidian University. His research interests include reconfigurable antenna, filtering antenna, microstrip filter, and compact circularly polarized antenna.

Long Li (M'06–SM'11) was born in Guizhou province, China. He received the B.E. and Ph.D. degrees in electromagnetic fields and microwave technology from Xidian University, Xi'an, China, in 1998 and 2005, respectively.

He joined the School of Electronic Engineering, Xidian University in 2005 and was promoted to Associate Professor in 2006. He was a Senior Research Associate in the Wireless Communications Research Center, City University of Hong Kong, Hong Kong, in 2006. He received the Japan Society for Promotion of Science (JSPS) Postdoctoral Fellowship and visited Tohoku University, Sendai, Japan, as a JSPS Fellow from November 2006 to November 2008. He was a Senior Visiting Scholar in the Pennsylvania State University from December 2013 to July 2014. He is currently a Professor in the School of Electronic Engineering, Xidian University. His research interests include metamaterials, computational electromagnetics, electromagnetic compatibility, novel antennas, and microwave devices design.

Dr. Li received the Nomination Award of National Excellent Doctoral Dissertation of China in 2007. He won the Best Paper Award in the International Symposium on Antennas and Propagation in 2008. He received the Program for New Century Excellent Talents in University of the Ministry of Education of China in 2010. He received the First Prize of Awards for Scientific Research Results offered by Shaanxi Provincial Department of Education, China, in 2013. He is a Senior Member of the Chinese Institute of Electronics.